The Libyan Journal of Science (An International Journal): Volume 19A, 2016

Computer Simulation of One Dimension Spin Echo Sequence for Magnetic Resonance Imaging

Nadia Gedafi, Zohra Arbi[1], Mohamed Mansor[2] and Taher Abuain[3]

Physics Department, University of Tripoli, P. O. Box 13402, Tripoli Libya, Libya
[1]Za8554186@gmail.com
[2]drmohmansor@Yahoo.com
[3] abuaint@Yahoo.com

Abstract

Magnetic Resonance Imaging MRI, using the Spin Echo method is studied here. A computer simulation for this method is presented for one dimension. The influence of the spin Echo Sequence is shown and its relation to different parameters such as repetition time TR, Echo time TE, relaxations times T1, T2, and the proton density PD of different tissues are studied. This study is useful for teaching purposes as well as for clinical applications.

Keywords: Spin Echo Simulation; MRI Simulation; Spin Sequence Simulation

المستخلص

استعمل في هذه الدراسة التصوير بالرنين المغناطيسي MRI بطريقة صدى البرم حيث تم تقديم محاكاة بالحاسوب في بعد واحد لهذه الطريقة. تم عرض تأثير تتابع صدى العزوم وعلاقته بالبارمترات المختلفة مثل زمن الاعادة وزمن الصدى وزمن الاسترخاء T1 و T2 وكثافة البروتون ، لانسجة مدروسة مختلفة. تصلح هذه الدراسة للاستعمالات التدرسية إضافة إلى التطبيقات السريرية (الإكلينيكية).

Introduction

Magnetic Resonance Imaging has been the subject of research for the last three decades [1-5]. The MRI scanners were first introduced in hospitals in the year 1982 [6]. Since then MRI has been developed and we see a wide use of these scanners in the world nowadays. In Libya, however, the first scanner was installed

Accepted for publication: 19/7/2016

at Central Hospital in 2005.

Many workers [7-9] presented computer simulations in order to understand and grasp the way MRI works. This is very important for developing and designing MRI scanners in order to achieve clear image in short time which helps diagnose certain diseases. In this study we have chosen the Spin Echo sequence because it is simple, and involves only two radio frequency pulses, the 90^o and the 180^o pulse.

Also the study is done for one dimension phantom as an attempt to understand the Spin Echo method and how different parameters are related to each other in controlling the enhancement and the contrast of images. We hope that this study will be extended to two dimensions where we can see the effect of these parameters on the images in two dimensions.

Theory

MRI imaging is based on relaxation of the magnetization introduced in tissue by an external magnetic field. Therefore, development of magnetization with time is of extreme importance to understand the theory of MRI imaging.

Bloch et al. [10] described, classically, the behavior of volume magnetization $\boldsymbol{M}$ under the influence of external magnetic field $\boldsymbol{B}$ by an equation known as Bloch equation [11, 12]:

$$\frac{d\boldsymbol{M}}{dt} = \gamma\,(\boldsymbol{M} \times \boldsymbol{B}) \qquad (1)$$

Where the vector $\boldsymbol{M}$ denotes the magnetization vector, γ is the gyro magnetic ratio which is $2\pi(42.6\times10^6)$(rad /sec T) for protons (spin ½), and the vector $\boldsymbol{B}$ is the local magnetic field. This magnetic field is the sum of all fields; the main external field $\boldsymbol{B}_0$ which is constant in the **k** direction**,** and the gradient of fields $\boldsymbol{G}$ which are linear on position and have the same direction as the main field direction**;** the radio frequency pulse field $\boldsymbol{B}_1$, and $\delta\,\boldsymbol{B}$ the field inhomogeneousity. The equation, thus, can be written as:

$$\frac{d\boldsymbol{M}}{dt} = \gamma\,\boldsymbol{M} \times (\,\boldsymbol{B}_0 + \delta\,\boldsymbol{B} + \boldsymbol{k}(\boldsymbol{G}.\boldsymbol{r}\,) + \boldsymbol{B}_1) \qquad (2)$$

This Equation shows that the change of magnetization with time ($\frac{d\boldsymbol{M}}{dt}$) is always perpendicular to $\boldsymbol{M}$, hence it represents rotation and precession of $\boldsymbol{M}$ in space.

When introducing a rotating frame system (x' y' z') around the z-axis with an angular velocity ($\omega_0 = |\gamma \boldsymbol{B_0}|$), the effect of the field $\boldsymbol{Bo}$ is not seen and we only see the precession due to $\delta \boldsymbol{B}$, $\boldsymbol{G}.\boldsymbol{r}$ and $\boldsymbol{B}_1$, then the equation becomes:

$$\frac{d\boldsymbol{M}}{dt} = \gamma\ \boldsymbol{M} \times (\ \ \delta \boldsymbol{B}\ + \boldsymbol{k}(\boldsymbol{G}.\boldsymbol{r}\ ) + \ \boldsymbol{B}_1\ ) \qquad (3)$$

Since in our study we do not deal with artifacts, we shall neglect the field inhomogeneousity and susceptibility effects, $\delta \boldsymbol{B}$, and keep only the *x*' and *y*' components of the radio frequency of interest. The equation could be written either in a vector or matrix form, respectively, as follows:

$$\frac{d\boldsymbol{M}}{dT} = \gamma \begin{vmatrix} \boldsymbol{i} & \boldsymbol{j} & \boldsymbol{k} \\ M_{x'} & M_{y'} & M_{z'} \\ B_{1x'} & B_{1y'} & \boldsymbol{G}.\boldsymbol{r} \end{vmatrix} \qquad (4)$$

$$\frac{d\boldsymbol{M}}{dT} = \gamma \begin{pmatrix} 0 & \boldsymbol{G}.\boldsymbol{r} & -B_{1y'} \\ -\boldsymbol{G}.\boldsymbol{r} & 0 & B_{1x'} \\ B_{1y'} & -B_{1x'} & 0 \end{pmatrix} \begin{pmatrix} M_{x'} \\ M_{y'} \\ M_z \end{pmatrix} \qquad (5)$$

The last form describes the magnetization vector in the rotating frame of reference (x' y' z'). In the equilibrium situation (saturation) the magnetization vector is parallel to the main magnetic field and has only a longitudinal component.

In non-equilibrium situation two processes exist that lead the magnetization back to equilibrium. One of these is spin-spin relaxation with characteristic decay time T_2 that causes the decrease in transverse magnetization M_T perpendicular to the main magnetic field; this can be described by exponential manner:

$$\frac{dM_T}{dt} = -\frac{M_T(t)}{\mathrm{T2}} \qquad \text{or} \qquad M_T(t) = M_T(0)\exp(\frac{-t}{\mathrm{T2}}) \qquad (6)$$

The other process is the relaxation of the longitudinal magnetization to its equilibrium values M_0 due to spin-lattice relaxation with a characteristic time T_1. This is given by a slightly different equation:

$$\frac{dM_z}{dt} = -\frac{M_z(t)-M_0}{\mathrm{T1}} \quad \text{or} \quad M_z(t)-M_0 = (M_z(0)-M_0)\ \exp(\frac{-t}{\mathrm{T1}}) \qquad (7)$$

If we include these processes, the Bloch matrix equation becomes:

$$\frac{d\boldsymbol{M}}{dT} = \begin{pmatrix} \frac{-1}{\mathrm{T2}} & \gamma\, \boldsymbol{G}.\boldsymbol{r} & -\gamma B_{1y'} \\ -\gamma \boldsymbol{G}.\boldsymbol{r} & \frac{-1}{\mathrm{T2}} & \gamma B_{1x'} \\ \gamma B_{1y'} & -\gamma B_{1x'} & \frac{-1}{\mathrm{T1}} \end{pmatrix} \begin{pmatrix} M_{x'} \\ M_{y'} \\ M_z \end{pmatrix} + \begin{pmatrix} 0 \\ 0 \\ \frac{M_0}{\mathrm{T1}} \end{pmatrix} \qquad (8)$$

In the absence of radio frequency pulse, the magnetization vector rotates (precesses) around the main magnetic field (z-axis) which is described by:

$$\frac{d\boldsymbol{M}}{dT} = \begin{pmatrix} \frac{-1}{\mathrm{T2}} & \gamma\, \boldsymbol{G}.\boldsymbol{r} & 0 \\ -\gamma \boldsymbol{G}.\boldsymbol{r} & \frac{-1}{\mathrm{T2}} & 0 \\ 0 & 0 & \frac{-1}{\mathrm{T1}} \end{pmatrix} \begin{pmatrix} M_{x'} \\ M_{y'} \\ M_{z'} \end{pmatrix} + \begin{pmatrix} 0 \\ 0 \\ \frac{M_0}{\mathrm{T1}} \end{pmatrix} \qquad (9)$$

For simplicity, the transfers magnetization is written in a complex notation;

$M_T(\mathrm{t}) = M_{x'} + \mathrm{j}\, M_{y'}$, where $\mathrm{j} = \sqrt{-1}$. Integration of these equations yields:

$$M_T(\mathrm{t}) = M_T(0)\ \exp\left(-j\gamma\, \boldsymbol{r}.\int_0^t \boldsymbol{G}(t')dt'\right) \exp\left(-\frac{t}{\mathrm{T2}}\right) \qquad (10)$$

The first exponential describes the precession in the (x'-y') plane, and the second exponential describes the relaxation, and for longitudinal magnetization:

$$M_z(t) - M_0 = (M_z(0) - M_0)\ \exp(\tfrac{-t}{\mathrm{T1}})\,. \qquad (11)$$

The Spin Echo Imaging Sequence

There are different methods for MRI Imaging, such as, Spin Echo, Fast Spin Echo, Gradient Echo and Inversion Recovery. Each method uses different imaging sequence of the RF pulses and the gradient fields that are applied during acquisition process. Of course each has advantages and disadvantages. For example the Spin Echo method enhances the Relaxation Time T1, T2, and PD (proton density) but cannot measure these relaxation times. Also it takes longer imaging time and is less affected by magnetic inhomogeneuosity. The Gradient Echo method also gives T1, T2, PD enhancement and is useful to measure the T2 relaxation time. It is also faster than the Spin Echo method. In the Spin Echo

method before a ninety pulse 90°, protons are aligned with the main magnetic field $\boldsymbol{B}_0$ resulting in a longitudinal magnetization M_z which is at its maximum value. When the 90^0 RF pulse is applied in the presence of $\boldsymbol{B_0}$ the longitudinal magnetization is rotated to a transverse plane where the protons precesses in phase around a vertical axis producing a transverse magnetization ($M_{x,y}$). Because of gradient fields, the spins will precess at different frequencies for different positions causing them to de-phase. However, during the de-phasing and at half Echo time TE/2 a 180^0, RF pulse is applied in the presence of the gradient field in the main field direction. The transverse magnetization is then flipped and starts to rephase again and the signal reachs its maxima at a time TE and an echo is obtained. After the echo event, the transverse magnetization starts to de-phase causing the echo to disappear. Figure 1 shows the spin echo pulse sequence timing and the transverse magnetization diagram.

For one dimension, the Spin Echo Equation (10) for one voxel becomes:

$$M_T = \left[M_0\, \rho(x_i)(1 - 2\, e^{-\frac{TR-\frac{TE}{2}}{T1\,(x_i)}} + e^{-\frac{TR}{T1(x_i)}}) \right] e^{-\frac{t}{T2\,(x_i)}}\, e^{\left[-j\gamma\, x_i \int_0^t G_x(t')dt'\right]} \quad (12)$$

Where $\rho\,(x_i)$ is the density in the specific position x_i which is a volume element called voxel and we shall note the term in brackets as the voxel amplitude magnetization VAM_i thus:

$$VAM_i = \left[M_0\, \rho(x_i)(1 - 2\, e^{-\frac{TR-\frac{TE}{2}}{T1\,(x_i)}} + e^{-\frac{TR}{T1(x_i)}}) \right] \quad (13)$$

TR is the repetition time for the imaging cycle.

The correction terms in $(1 - 2\, e^{-\frac{TR-\frac{TE}{2}}{T1\,(x_i)}} + e^{-\frac{TR}{T1(x_i)}})$ are due to repetition of signal excitation and the fact that the magnetization does not reach 100% saturation at the start of the next excitation pulse 90°. The total transverse magnetization which is simply the summation of the magnetizations of the different voxels at any later time t after the 90° pulse is given by:

$$M_T = \sum_i VAM_i\, e^{-\frac{t}{T2\,(x_i)}}\, e^{\left[-j\gamma\, x_i \int_0^t G_x(t')dt'\right]} \quad (14)$$

As the signal is proportional to the proton magnetization at each voxel, the total signal from all voxels will also be:

$$S \alpha \sum_i \ VAM_i \ . e^{-\frac{t}{T2(x_i)}} . e^{\left[-j\gamma x_i \ \int_0^t G_x(t')dt\prime\right]} \quad (15)$$

This equation is used for the Spin Echo simulation in this study. Although this study is for one dimension it is useful to describe the Spin Echo imaging cycle. Figure 2 shows that the cycle contains three regions. The left side shows the T1 contrast. For very small value of TR there is no contrast. The contrast is developed between the tissue, as TR increases the contrast increases then proton density contrast develops and it overcomes the T1 contrast. This is seen in the middle part of the imaging cycle.

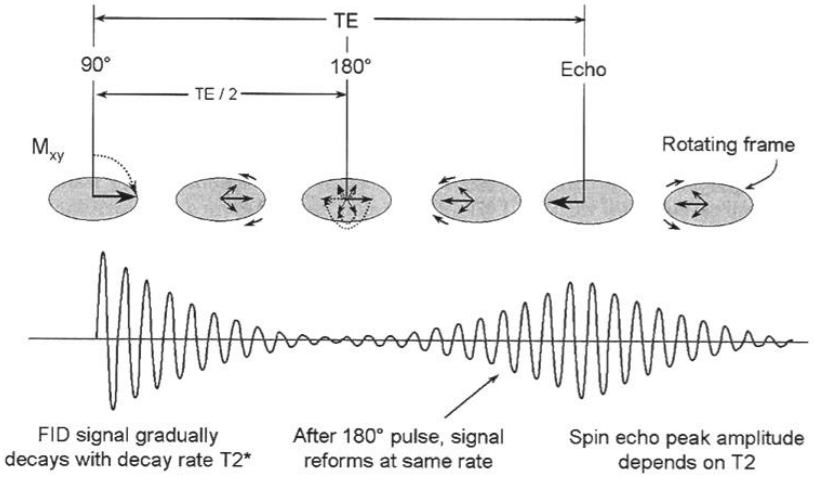

Figure 1**.** Spin echo pulse timing and diagram [12]**.**

The right side of the cycle is the T2 contrast appearing at long TR and as TE increases a good T2 contrast is achieved.

From the above we notice that for the T1 contrast TR must be short as well as TE. For proton density contrast TR must be long but TE is short, and for T2 contrast TR must be long and TE is also long TE. It was noticed that there could be a mixture of proton density, T1, and T2 contrasts. The disadvantage of the Spin Echo is that T2 effect always exists.

Results and Discussion

MathCAD software was used in this study. Three tissues were chosen to simulate the Spin Echo method. These are: White Matter (WM), a Gray Matter t(GM) and Cerebrospinal Fluid (CSF). Table 1, shows the T1, T2 and PD values

for these issues. Equation (15) is used for this calculation. Note that the transverse magnetization M_T (x_i) is for one variable (x_i), and hence the obtained signal is for one dimension. Fast Fourier transformation is used to transform the signal from the time domain to the frequency domain.

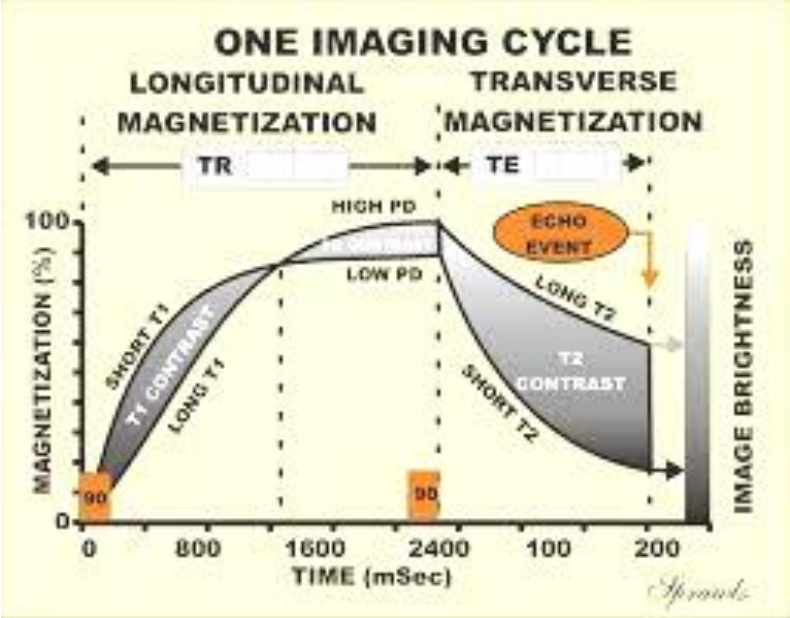

Figure 2. Contrast of imaging in Spin Echo cycle [13].

We divided the phantom linearly into a large number of voxels with small thicknesses. Each voxel has its own frequency because of the presence of gradient field. The spins in it are all in phase to each other, and hence it develops its own magnetization which will be called voxel amplitude magnetization VAM_i at position (x_i) just after the 90^o-pulse is applied which is given by the equation:

$$VAM_i = \left[M_0 \, \rho(x_i) . (1 - 2\, e^{-\frac{TR-\frac{TE}{2}}{T1(x_i)}} + e^{-\frac{TR}{T1(x_i)}}) \right]$$

We set M_0 always to the value of one, because it only depends on external field strength and temperature.

The main purpose of this study is to show how the different parameters T1, T2, TE, TR, and PD are related to imaging in the Spin Echo sequence. In particular how the TR and TE affect the T1, T2 and the proton density contrast of images.

Figure 3a shows the calculated echo signal intensity. A short echo time is selected; TE = 10 mSec and the repetition time is selected at TR = 300 mSec. The proposed proton density (the one dimension phantom) for the different tissue is shown in figure 3c. The solid line is for the chosen proton density (phantom) and the dotted line is the calculated voxel amplitude magnetization *VAM* just before the 90^o pulse is applied. We notice that the calculated VAM is less than the relative proton density PD which actually represent the saturated voxel magnetization at large TR, so this effect is T1 contrast. From the Figure 3b. we see that that the discrepancy between the WM and GM is weak. However the signal for the CSF is very low. Both figures 3b & c are in a good agreement with each other.

Table 1**.** Values of T1, T2 and relative PD for different tissues.

Tissues	T1(mSec)	T2(mSec)	PD
CSF	2400	160	1.0
WM	780	90	0.72
GM	920	100	0.84

Figure 3d shows the calculated image at the same echo time TE = 10mSec for TR =700 mSec. We notice from the figure that the discrepancy between the WM and GM increased and the signal for the CSF increased but still low indicating enhancement of T1 contrast in agreement with Figure 3e.

The repetition time is increased to a higher value TR=5000mSec, TR=9000 mSec and TR =12000mSec for the same short echo time TE = 10 mSec. We can see from figure 3g-j that VAM curve is closer to PD curve except for CSF which is close to GM. So at this small TE value the contrast between GM and CSF is very small as can be seen from Figure 3f. Increasing TR to 9000 mSec and higher the images, (Figure 3h-j) reflect proton density contrast as expected. Figure 3k shows complete proton density contrast for VAM and hence is reflected in the image.

The Echo time TE is increased to 30 mSec, and the repetition time is chosen for TR values of 300, 700, 9000 and 12000 mSec. We can see from the Figure 4b that for the short time TR=300 the VAM curve is low compared to the proton density PD and it increases as TR increases (Fig. 4d). Accordingly, at these TR values there is no significant contrast between the WM and GM, but for the CSF a clear contrast is shown, and hence T1 enhancement. Similar to TR in Figure 5&b,

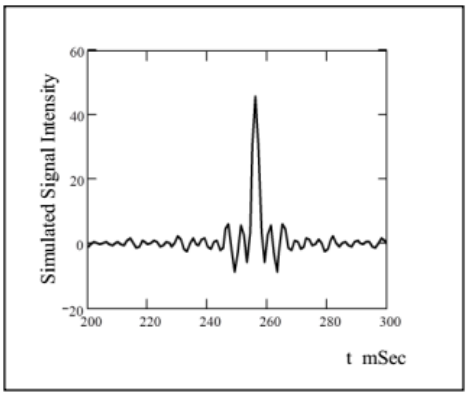

(a) Echo Signal Intensity TR = 300 mSec.

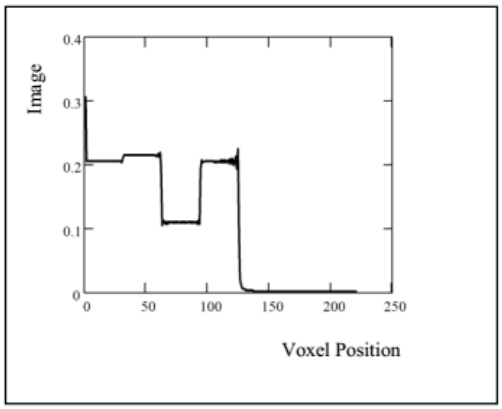

(b) TR = 300 mSec.

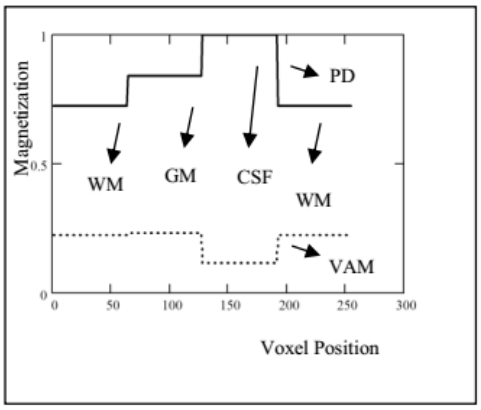

(c) TR = 300 mSec.

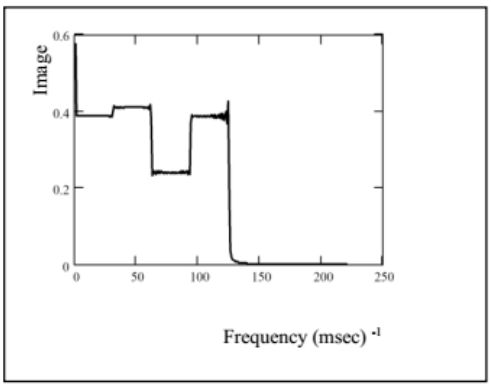

(d) TR = 700 mSec.

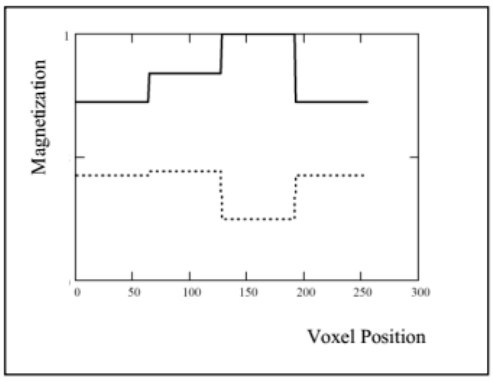

(e) TR = 700 mSec.

Figure 3. TE =10 mSec.

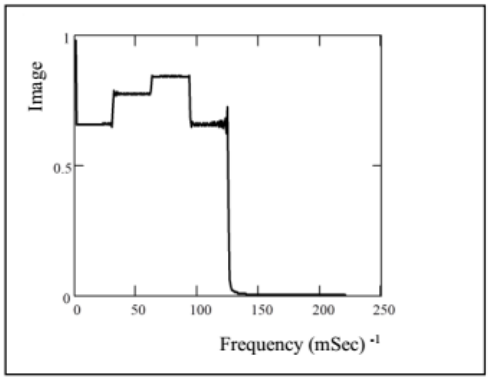

(f) TR = 5000 mSec.

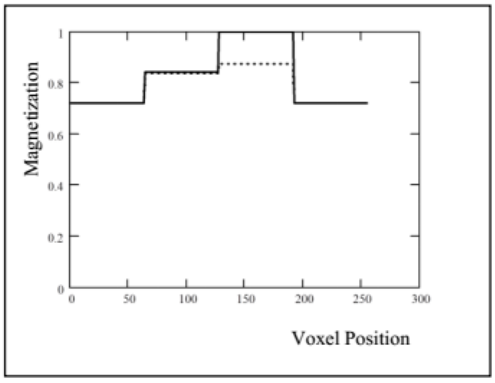

(g) TR = 5000 mSec.

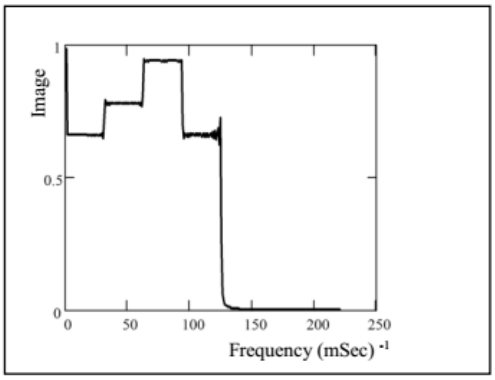

(h) TR = 9000 mSec.

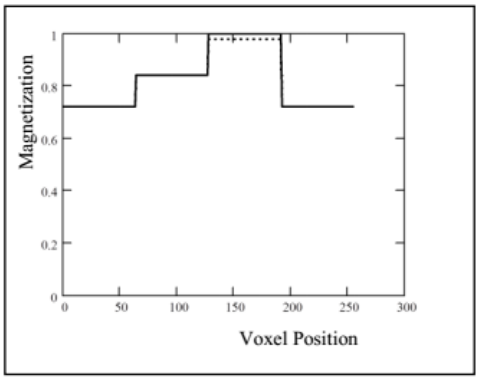

(i) TR = 9000 mSec.

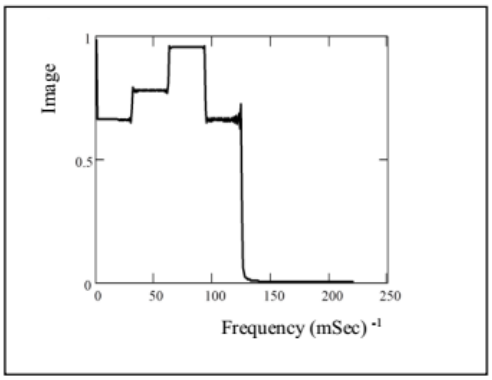

(j) TR = 12000 mSec.

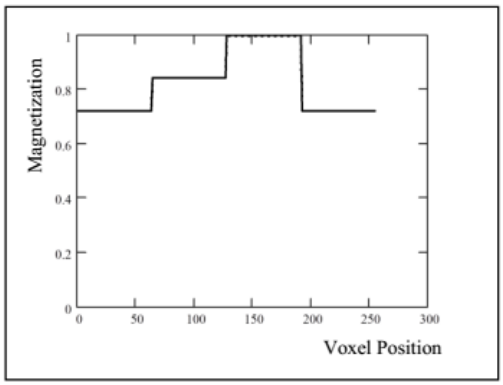

(k) TR = 12000 mSec.

Figure 3 (Cont.). TE =10 mSec.

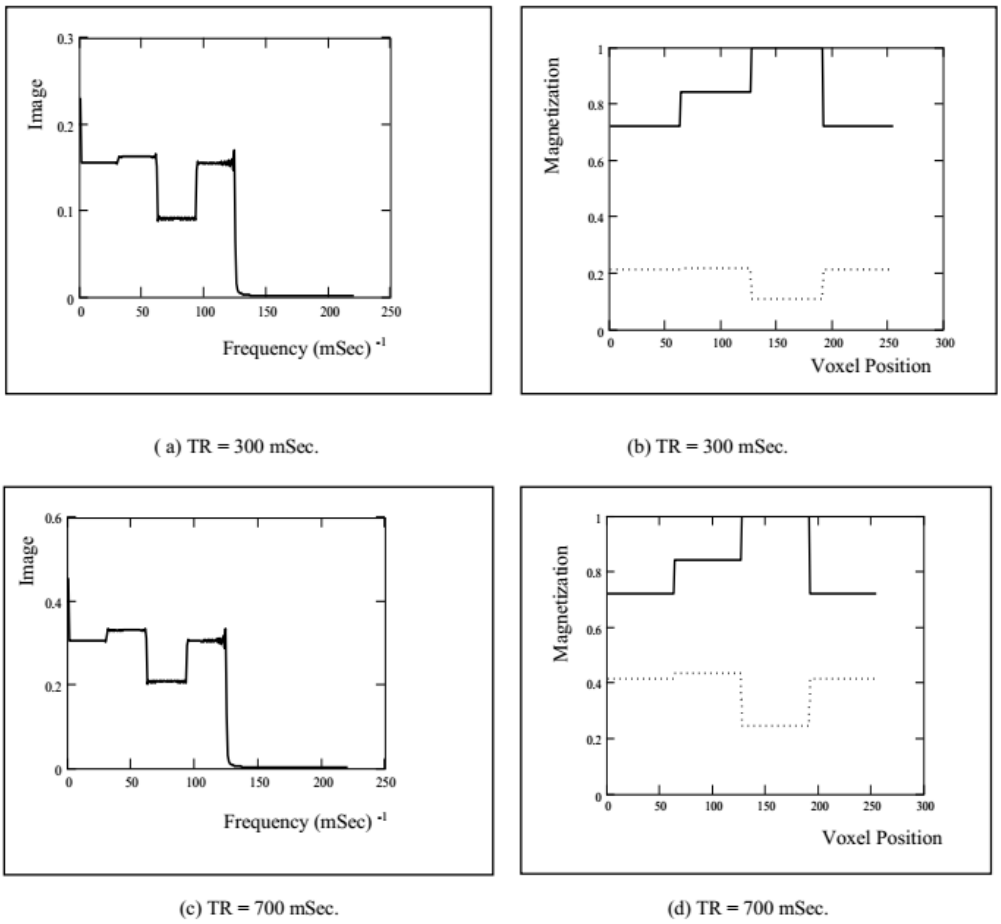

Figure 4. TE = 30 mSec.

TE is increased to 100 mSec and for short TR = 300 mSec we can see T1 contrast in the image between GM and WM with respect to cerebrospinal fluid. This emphasizes that a long TR time is necessary for the proton density and the CSF contrast. For higher TR=700 mSec less contrast results between WM and CSF because of competition between T1 and T2, even though in both cases VAM shows equality between GM and WM magnetization (Fig. 5d). For higher TR again clear T2 as well as PD contrast is shown in both VAM and images (Fig. 5f-g).

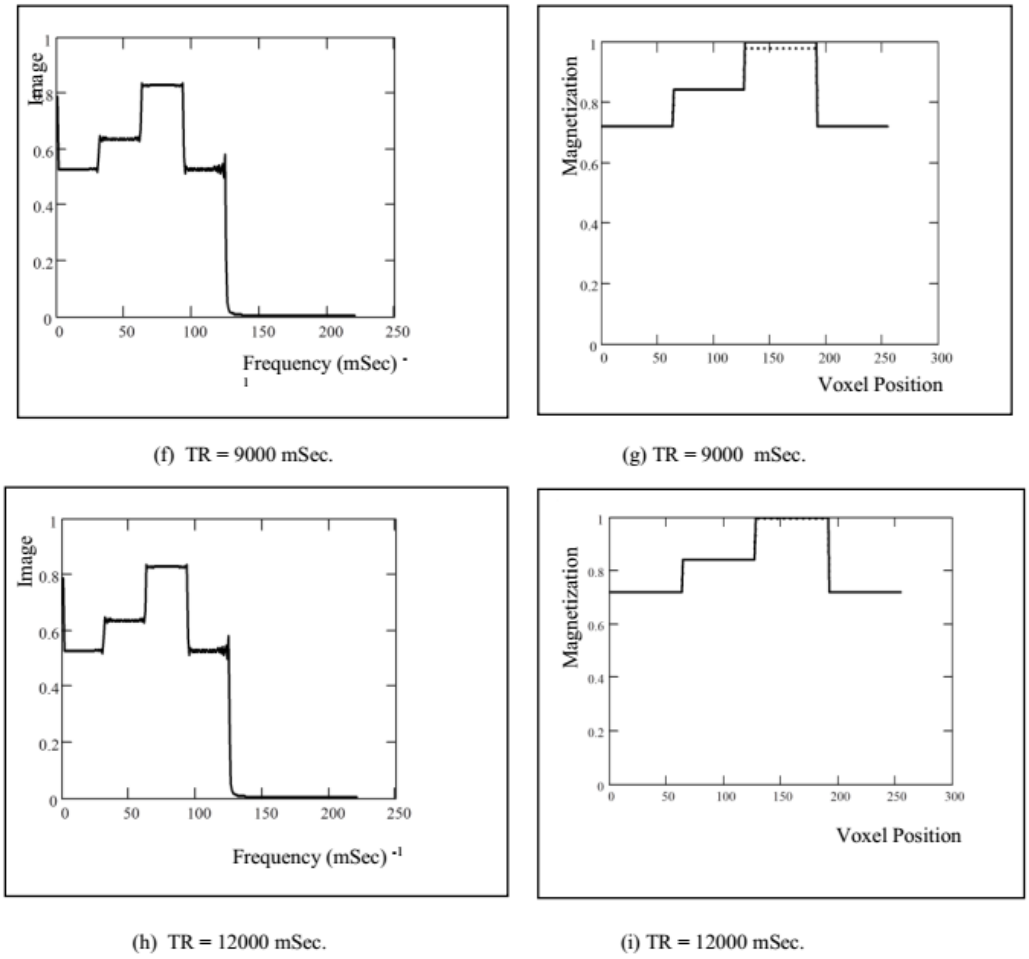

Figure 4. Continued TE = 30 mSec.

Relaxometry

Relaxometry is a method for the measurement of relaxation rates, which is based on the physical aspect of nuclear relaxation to the ground state after being excited by an RF pulse. This relaxation is produced by randomly occurring variation in the local magnetic strength. Immediately after the RF pulse, only protons spinning in phase can give rise to detectible signal, they become out of phase as they experience a slightly different magnetic field and then rotate at slightly different frequencies. This transverse magnetization de-coherence occurs both due to magnetic field inhomogeneity produced by the magnet (gradient field)

or by magnetic particles present in the tissue and due to movement of molecules in the tissue. Relaxometry may be used either by Spin Echo or by Gradient Imaging Echo sequences. Since our study is concerned with the former, we will represent how this analysis is used by studying the different parameters controlling the image contrast. The following equation is used for this analysis of a particular tissue:

$$M_T = \left[M_0 \, \rho(x_i)(1 - 2\, e^{-\frac{\mathrm{TR}-\frac{\mathrm{TE}}{2}}{\mathrm{T1}\,(x_i)}} + e^{-\frac{\mathrm{TR}}{\mathrm{T1}(x_i)}}) \right] e^{-\frac{t}{\mathrm{T2}\,(x_i)}}$$

This equation does not separate T1 and T2 contributions sufficiently to detect abnormality of tissues.

When repetition time is chosen short; TR=300 mSec, TR =700 mSec, TR= 1000 mSec and the Echo time is varied from TE= 0.0 To 60 mSec (Fig.e 6. a-c), the FAT signal is the highest, while the CSF is the lowest. The WM and the GM signals, however, are almost equal. This signal is suppressed by the T1 relaxation and we also notice that as TE increases the T2 supressim is present. The image, however, approaches the proposed one dimension phantom**.**

When the repetition time is chosen to be longer; TR = 5000 mSec (Fig. 6d), we notice that when TE is short (TE<20) mSec the FAT, GM, and WM signals approach the same value and there is no resolution for any tissue, while the CSF signal is still lower and it is enhanced among other tissues. This is because it has longer relaxation time T1 than other tissues. As TE increases to 40 mSec > TE >20 mSec, the signals from all tissues are close to each other and the resolution between the tissues is very weak because of T2 effect. At TR = 7000 mSec and TE>20 mSec the CSF signal is higher than other tissues and its enhancement increases while the Fat signal decreases. At this stage we reason that the enhancement due to the T2 relaxation is important. As the TR is increased to TR=12000 mSec (Fig. 6f), we conclude that at low TE the signals are equal for all tissues. The contrast should be due to the proton density and as the echo time increases we can see that CSF has the highest signal while the FAT has the lowest signal and it appears that the enhancement is due to the T2 relaxation time.

Conclusion

We conclude from this study that computer simulation is a good approach in doing research that needs sophisticated and expensive equipment. As we have seen in our case, we introduced the basis of the MRI research and particularly the Spin Echo Technique or Imaging.

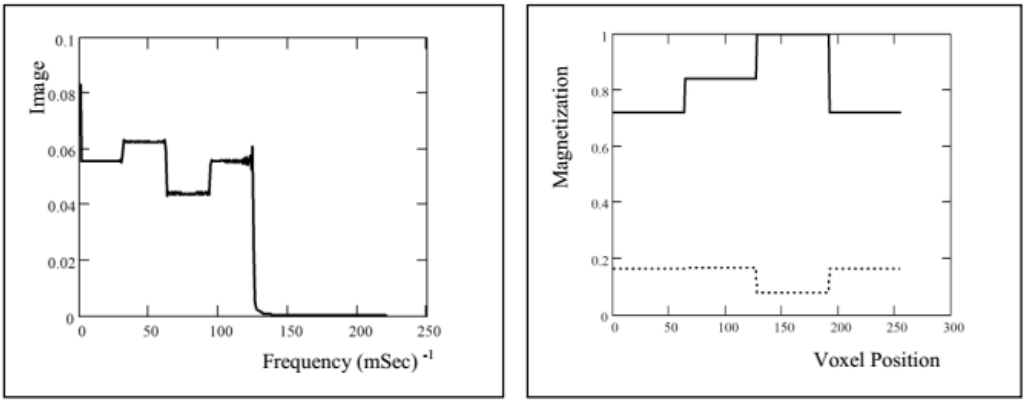

(a) TR = 300 mSec. (b) TR = 300 mSec.

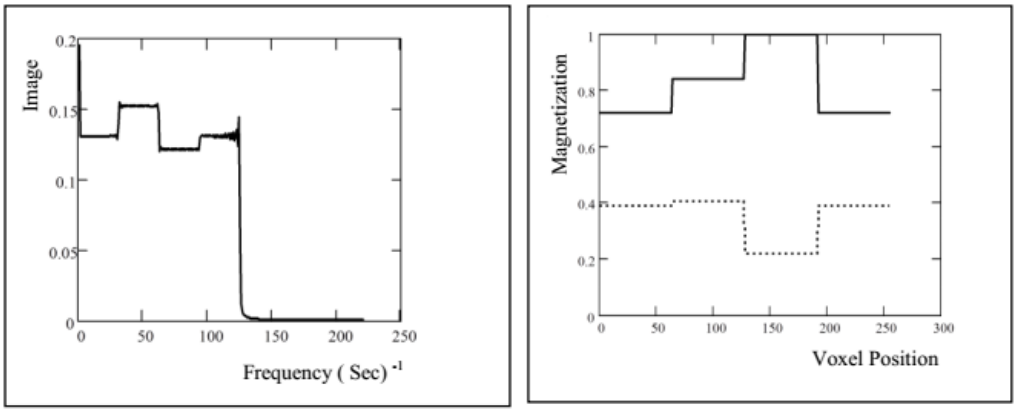

(c) TR = 700 mSec. (d) TR = 700 mSec.

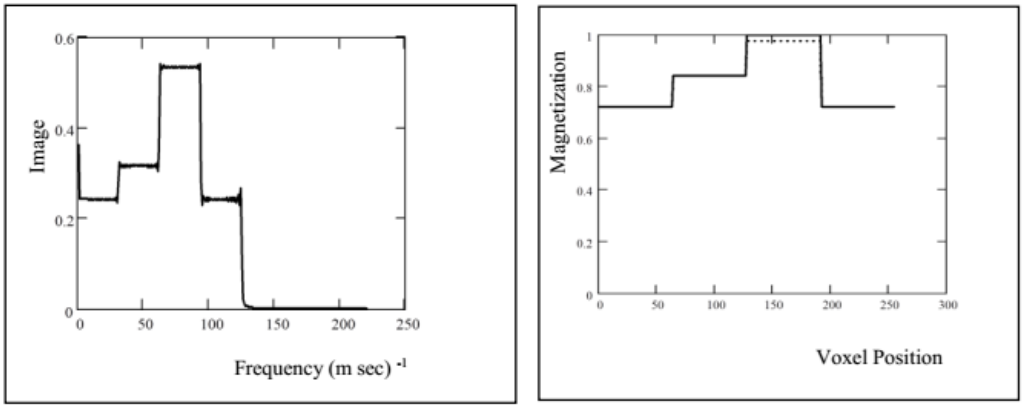

(e) TR = 9000 mSec. (f) TR = 9000 mSec.

Figure 5. TE = 100 mSec.

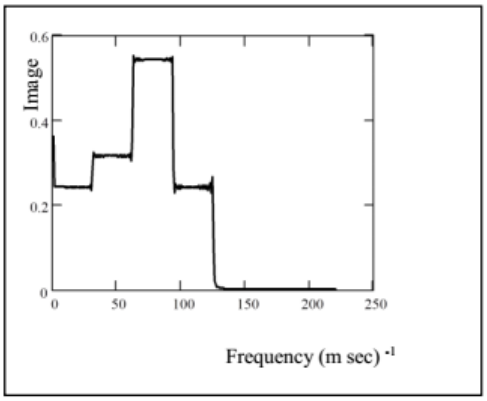

(g) TR = 12000 mSec.

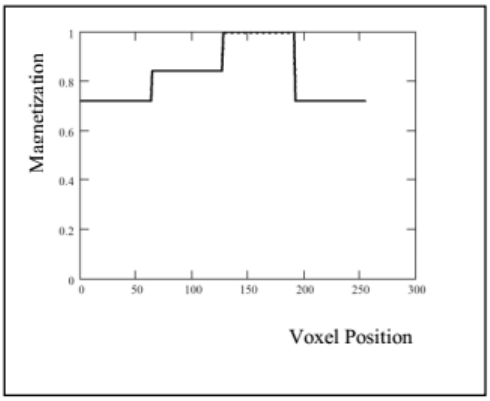

(h) TR = 12000 mSec.

Figure 5 (Cont.). TE = 100 mSec.

In this study we found the relationship between the different factors that control the enhancement of the different tissues relaxation times on the type of the image or image contrast. We found that for the contrast of the relaxation time T1 or T1 weighted image (to show the fat tissue) you need to use a short Echo time TE and short repetition time TR. For the proton density contrast (to show gray matter, liver or spleen) you need to use a short Echo time TE and long repetition time TR. For contrast of the T2 relaxation time or T1 image (to show cerebrospinal fluid CSF), the use of a long time TE as well as a long TR are needed.

We would like to extend this research to two dimensions where we can see the image and learn more about the Spin Echo imaging and how it is affected by the gradient field as well.

Acknowledgements

Dr. T. Abuain and Dr. M. Mansor are grateful to Prof. David Lurie who gave them the chance to visit and mingle with his MRI Group at Aberdeen University. This gave us the chance to start the MRI research at Tripoli University. We also thank the Aberdeen MRI Group for the over welcome and for allowing us to participate with them in the research meetings.

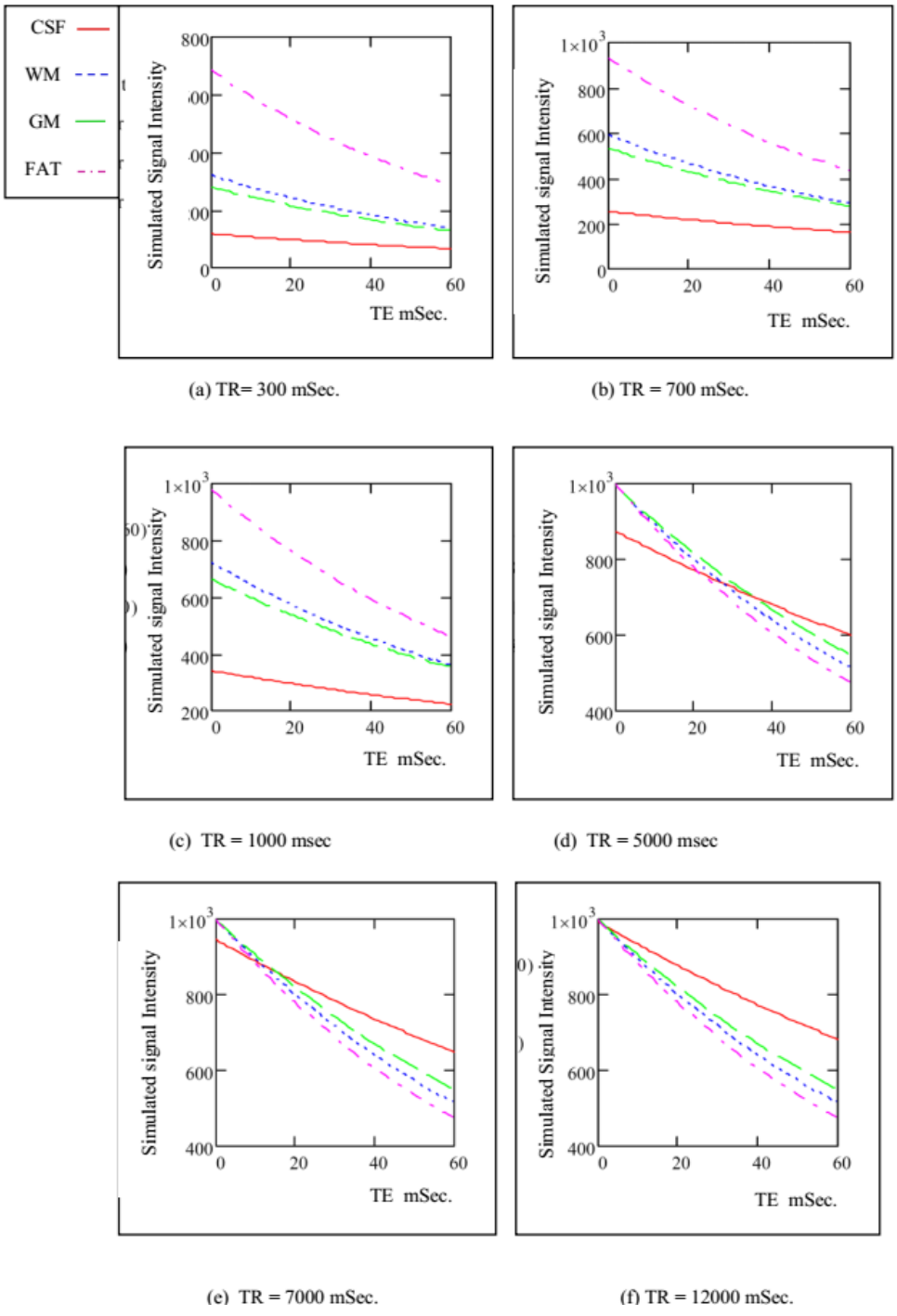

Figure 6**.** Simulated signal intensity versus Echo time for different repetition time.

References

[1] Michell, M. R., Tarr, R. W., Conturo, T. E., Partain C. L. James, A. E. and Lean, C. (1986). Spin echo technique selection: Basic principle for choosing MRI pulse sequence timing intervals, RadioGraphics, **6**, 245-260.

[2] Haase, A. (1990). Snapshot flash MRI, application to T1, T2 and chemical-shift imaging. Magnetic Resonance in Medicine,**13**,77-89.

[3] Pauly, J., Nishmura, D. T. and Macovski, A. (1989). A-k space analysis of small-tip-angle excitation. Journal of Magnetic Resonance, **81**,43-56.

[4] Lurie, D. (1983). A sysmantec design procedure for selective pulse in NMR imaging. Magnetic Resonance Imaging, **3**, 235-243.

[5] Viniski, S., Albert, S., Mitchell, D. G. Tasciyan, T. A. and Rifkin, M. D. (1992). Partial angle inversion recovery (pair) MR Imaging: Spin echo and snapshot implementation. Magnetic Resonance Imaging, **10 (2)**, 207-215.

[6] Lecture Notes (2007). Magnetic Resonance Imaging. University of Aberdeen, Scotland, England.

[7] Benoit, H., Catin, H., Collwet, G., Bellarousi, B., Saint-James, H. and Odel, C. (2004). The SIMRI project: A versatile and interactive MRI simulator. Journal of Magnetic Resonance, **173**, 97-115

[8] Carnerio, A. A. O, Vila, G. R., et al. (2006). MRI relaxometry: methods and applications. Brazilian Journal of Physics, **36** (1a), 1-13.

[9] Broche, L. M, Ross, P., James, M., Pine, K. J. and Lurie, D. J. (2013). Rapid multi-field T_1 estimation algorithm for fast field-cycling MRI. Journal of Magnetic Resonance, 1-17.

[10] Bloch, F., Hanson, W. and Packard, M. E. (1946). Nuclear induction. Phys. Rev., **69**, 127.

[11] Marinus, T., Vlaardingerbroek, J. (1995). Magnetic Resonance Imaging: Theory and Practice, 2d edition, Springer,Berlin, 65 p.

[12] http://medradresource.blogspot.com/2012/11/what is spin echo-used for.in.nmr.html.

[13] Sprawls, P. (2000). Magnetic Resonance Imaging: Principles, Methods, and Techniques, 1st edition, Medical Physics Publishing, Madison, Wisconsin, 62p.